Photoionization spectroscopy for laser extraction of the radioactive isotope ^{177}Lu

A. B. D'yachkov[1] · V. A. Firsov[1] · A. A. Gorkunov[1] · A. V. Labozin[1] · S. M. Mironov[1] · V. Y. Panchenko[1] · A. N. Semenov[1] · G. G. Shatalova[1] · G. O. Tsvetkov[1]

Abstract The hyperfine structure of the $5d6s^2$ $^2D_{3/2} \rightarrow 5d6s6p$ $^4F_{5/2}$ transition of the radioactive isotope ^{177}Lu has been investigated by laser photoionization spectroscopy. Measured spectra permitted the determination of hyperfine magnetic dipole constants and electric quadrupole constants for ground and excited state as well as the isotope shift of the ^{177}Lu isotope. The data obtained were used to confirm the selective photoionization of ^{177}Lu from a neutron-irradiated sample that initially had a natural isotope composition. A concentration for ^{177}Lu of 50 % was achieved, and the photoionization efficiency was estimated as suitable for technological application.

1 Introduction

An increased interest in the isotope ^{177}Lu over the last decade has been associated with its growing use in cancer treatment owing to its special nuclear properties: a β^- decay half-life of 6.7 days, a low energy of 0.13 MeV, a short absorption path for the beta emission (<2 mm), and γ-emissions suitable for imaging [1–4]. Various therapies require different specific activities of ^{177}Lu. In particular, ^{177}Lu with a concentration >20 % (specific activity >740 GBq/mg) is used in peptide receptor radionuclide therapy [5]. Given that natural lutetium contains only ^{175}Lu (97.4 %) and ^{176}Lu (2.6 %), ^{177}Lu must be produced artificially. Current production methods use either highly enriched isotopes of ^{176}Lu (direct route) or ^{176}Yb (indirect route), which are irradiated in a nuclear reactor with further radiochemical processing. The enriched material use efficiency is very low, and even for the direct route the efficiency does not exceed 25 % [6]. Another possible production route, proposed in this work, is to use a neutron capture reaction ^{176}Lu $(n,\gamma) \rightarrow$ ^{177}Lu, where natural lutetium metal is irradiated in a nuclear reactor. After irradiation, the lutetium target consists of the natural isotopes ^{175}Lu, ^{176}Lu, and ^{177}Lu together with the nuclear isomer ^{177m}Lu. The concentration of ^{177}Lu, which depends on the neutron flux and the spectral characteristics, is typically <0.1 %. For medical applications, ^{177}Lu needs to be extracted from the mixture and this step can be performed by atomic vapor laser isotope separation technology (AVLIS technology) [7–9]. It is considered that this approach involving isotope separation at the final stage of ^{177}Lu radionuclide production is promising, particularly from the standpoints of efficiency and low-waste technology.

It should be noted that laser isotope separation has been achieved for indirect ^{177}Lu production [10]. Using this laser technology, the authors succeeded in extracting ^{176}Yb enriched up to 97 % from natural ytterbium.

A three-step selective photoionization scheme (most typical for AVLIS) for lutetium has recently been proposed and investigated for a natural isotope mixture [11] (Fig. 1). The scheme was used successfully for ^{176}Lu extraction from a natural isotope mixture. Despite a small isotope shift (−388.8 MHz) [12], ^{176}Lu could be separated from ^{175}Lu. Some hyperfine structure (HFS) components of ^{176}Lu and ^{175}Lu were sufficiently separated from each other, thus permitting selective and efficient photoionization of ^{176}Lu. In this way, a weight amount of ^{176}Lu with a concentration of about 70 % was prepared.

✉ G. O. Tsvetkov
glebtsvetkov@mail.ru

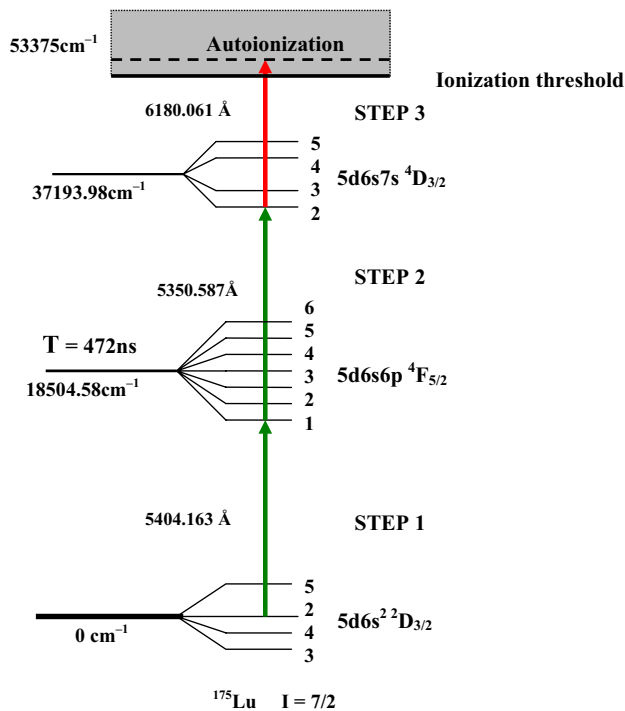[1] National Research Centre "Kurchatov Institute", Kurchatov sq. 1, Moscow, Russia 123182

Fig. 1 Three-step scheme for ^{175}Lu photoionization suitable for CVL pumped dye lasers

The present study is concerned with application of the ^{177}Lu extraction scheme to neutron-irradiated natural lutetium. The possibility for this process is critically dependent on whether there are HFS ^{177}Lu components that may be used for selective photoionization. The HFS spectroscopy of the optical transition at 451.9 nm for ^{177}Lu was explored [13], but this transition was not applicable to conventional AVLIS with dye lasers pumped by copper vapor lasers (CVL). Therefore, the structure of the transition from the ground state $5d6s^2$ $^2D_{3/2}$ to the excited state $5d6s6p$ $^4F_{5/2}$ at 540.4 nm (also further wavelengths in the vacuum) was investigated. Despite data on the HFS of the ^{177}Lu ground state being available [13–15], there is no information on isotope shifts and hyperfine interaction constants for the $5d6s6p$ $^4F_{5/2}$ level, hence the raison d'être for this work.

2 Experimental

Research was performed at a purpose-built facility for spectroscopic measurements. The instrumentation featured narrow collimated atomic beams, and specialized equipment was used for determination of photoion isotopic composition following laser resonance selective photoionization. This technique and setup are quite similar to conventional resonance ionization spectroscopy setups described elsewhere [10, 16, 17]. The facility included a vacuum chamber with pumping system, a tantalum oven mounted inside the chamber, a quadrupole mass spectrometer, and photoion and fluorescence registration units. The CVL pumped dye laser system consisted of three single-mode master oscillators and two dye amplifiers. The master oscillators were constructed on the grazing incidence diffraction grating scheme [18]. The laser dye, pyrromethene-556 pumped with the 510.7-nm CVL component, was applied on the first and second steps (Fig. 1). Sulforhodamine-640 pumped by the 578.3-nm CVL component was used on the third step. Master oscillators were able to scan the radiation wavelength by changing the drive voltage on the piezoelectric supports of the cavity-dispersive elements. High-precision meters (LM-007, Laser 2000 GmbH) provided laser wavelength measurements with an absolute accuracy of 0.0005 Å and served also as stabilized etalons for active wavelength stabilization of master oscillators. Dye amplifiers [19] were used to increase power at the second and third steps. Three output laser beams were expanded to a diameter of 12 mm and then collimated. Semitransparent and dichroic mirrors were used to combine the radiation from the three dye lasers into one beam. The second- and third-step laser pulses were time delayed by 25 ns with respect to the first laser step pulse to avoid the effect of multiphoton processes on wavelength determination. Given that the lifetime of the $5d6s6p$ $^4F_{5/2}$ level is 472 ns [20], the second and third laser radiation affects the atoms in the excited state after termination of the first laser step pulse. The performance parameters of the laser system are presented in Table 1.

The 12-mm-diameter, three-color laser beam was transmitted through a 2-mm diaphragm and directed into the mass spectrometer.

Table 1 Performance parameters of the laser system

	Scanning range (Å)	Maximum average power (W)	Bandwidth (FWHM) (MHz)	Pulse duration (FWHM) (ns)	Pulse repetition rate (kHz)	Amplified spontaneous emission (%)
λ_1	5403.95–5404.18	0.1				0.3
λ_2	5350.57–5350.65	1	100	20	10	0.3
λ_3	6180.03–6180.11	4				0.6

Five milligrams of natural lutetium metal was irradiated by a 1.5×10^{13} 1/cm^2 s thermal neutron flux for 1 day, and after a decay time of 1 week, the irradiated sample was loaded into the tantalum oven. The concentration of radioactive ^{177}Lu atoms, as determined by gamma spectroscopic analysis, was 10^{-5}. Vaporized lutetium atoms (several milligrams per hour) passed through the diaphragm system and formed an atomic beam (3° divergence angle) that was orthogonal to the laser beam. The estimated Doppler broadening was ~100 MHz. The laser beam intersected the atomic beam directly within the ionization (electron impact) chamber of the mass spectrometer. The intersection region had the shape of a cylinder with a diameter and length of 2 mm. Photoions were detected by a secondary electron multiplier, and fluorescent photons were measured by a photomultiplier located on an ion-optical spectrometer axis in a direction opposite to the photoion flow (Fig. 2). The fluorescence registration system had low sensitivity and could not detect ^{177}Lu fluorescence. This system was used for measuring [175]Lu HFS. Control of the laser system and data recording were accomplished on line, and this allowed the experiment to be completed in 1 h.

To measure the ^{177}Lu photoion spectrum, the first wavelength was scanned, while the second- and third-step wavelengths were fixed and stabilized. The whole HFS structure of the transition cannot be measured in one scan as the wavelengths of the second and third step are different for each HFS component. Each scan included one or several HFS resonances, which are close to each other and can be measured when the second- and third-step laser wavelengths are fixed. For different scans, the wavelengths of the second and third step were roughly adjusted to maintain the ion signal value. The photoion signal versus wavelength of the first transition is shown in Fig. 3. Because of the imperfections in the second and third wavelengths tuning mentioned above, the amplitude of the components did not represent the real oscillator strength.

3 Results and discussion

The experimental data permitted calculation of the ground- and excited-state hyperfine interaction constants and the center of gravity (CG) energy for the $5d6s6p$ $^4F_{5/2}$ state based on the expression:

$$E + \Delta_{F'} - \Delta_F = \frac{1}{\lambda_{FF'}}, \tag{1}$$

where E (cm^{-1}) is the CG energy of the excited level (zero for ground state), Δ_F and $\Delta_{F'}$ (cm^{-1}) are the low- and upper-level hyperfine splitting, and $\lambda_{FF'}$ (cm) is the transition wavelength. The center of each line was determined by Voigt line shape fitting performed using packet PAW of the
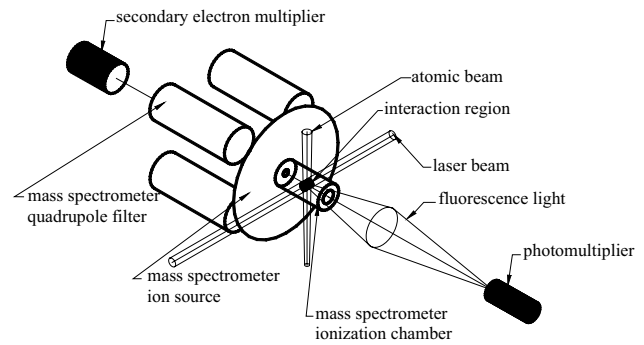

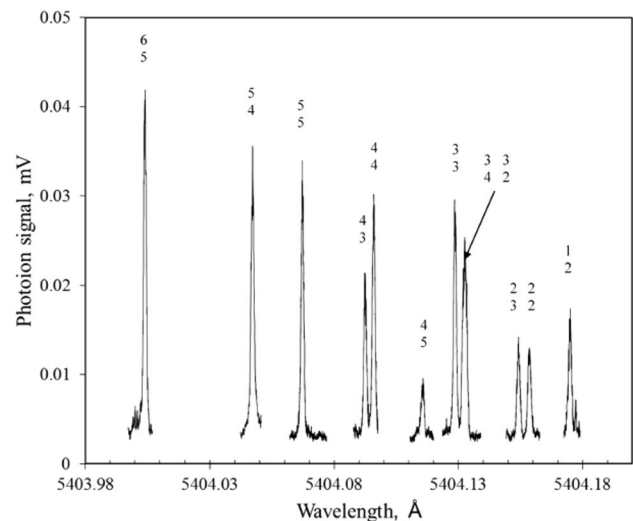**Fig. 2** Photoion current and fluorescence registration scheme

Fig. 3 Hyperfine structure of the $5d6s2$ $^2D_{3/2} \rightarrow 5d6s6p$ $^4F_{5/2}$ transition. The low number F is the ground-state total angular momentum of atom, while the upper number F' is the momentum of the excited state. All transitions were identified except the $4 \rightarrow 3$ and the $2 \rightarrow 3$ transitions, which were not resolved. The *arrow marks* these resonances

CERN library [21]. The best fit found corresponded to 10 $(+10; -5)$ MHz Lorentzian and 125 (±10) MHz Gaussian widths (confidence level of 95 %) and was the same for all peaks (Fig. 4).

The constants for the hyperfine magnetic dipole and electric quadrupole interactions of the excited A_e, B_e, and ground states A_g, B_g are included with a linear relationship in the equations for $\Delta_{F'}$ and Δ_F [22]. The A- and B-factors as well as the CG energy found by the least square fit are listed in Table 2.

The ^{177}Lu ground-state constants obtained in this study coincided with published values [13–15] within experimental error. It is possible to compare the measured ^{177}Lu excited-state constants with the estimates using the appropriate [175]Lu values [23]. Actually, apart from a small hyperfine anomaly, the ratio of the ^{177}Lu and [175]Lu

Fig. 4 Measured line shape of ^{177}Lu $5d6s2$ $^2D_{3/2} \rightarrow 5d6s6p$ $^4F_{5/2}$ 5–6 transition ($\lambda = 5404.0040$ Å) and the Voigt fitting function (Gaussian FWHM was 115 MHz and Lorentzian FWHM was 15 MHz)
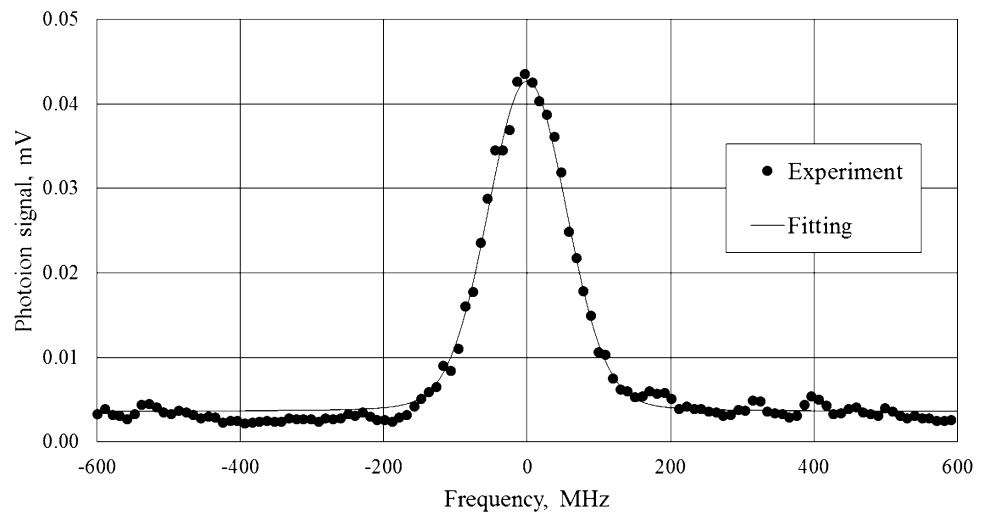

Table 2 Experimental results and estimates of HFS constants and isotope shifts for $^{175-177m}$Lu isotopes

Isotope	Nuclear spin	A_g (MHz)	A_e (MHz)	B_g (MHz)	B_e (MHz)	E (cm^{-1})	Isotope shift from ^{175}Lu (MHz)	References
^{175}Lu	7/2	199 (9)	990 (13)	1510 (50)	1058 (130)	18504.586 (2)	–	This work
^{175}Lu	7/2	194.4 (7)	987.35 (12)	1509 (6)	1117.9 (2.0)	18504.58	–	[13, 23, 26]
^{176}Lu	7	137.9 (0.6)	698.25 (15)	2132 (4)	1572.2 (3.0)		−388.8 (11)	[12, 23, 24]
^{177}Lu	7/2	196 (2)	990 (2)	1457 (37)	1058 (44)	18504.546 (1)	−1199 (89)	This work
^{177}Lu	7/2	194.9 (6)		1467 (5)				[13]
^{177}Lu	7/2		990.22		1084.58		−1147	Estimate
^{177m}Lu	23/2	61.2 (3)		2472 (11)				[13]
^{177m}Lu	23/2		311		1829		−815	Estimate

constants was equal to the ratio of the known nuclear magnetic μ_I/I factors for A_e (μ_I—nuclear magnetic moment, I—nuclear spin) and the quadrupole moments for B_e of these isotopes [13]. The measured values are in good agreement with estimates (Table 2, row 4 and 6). It was also possible to compare the ^{175}Lu and ^{177}Lu isotope shifts measured and estimated. In heavy atoms, the isotope shift is mainly caused by differences in nuclear charge density distribution (field shift). For the transition of interest, $5d6s^2 \rightarrow 5d6s6p$, the isotope shift is almost completely a field shift because the normal and the specific mass shifts are small and do not exceed ~20 MHz [24]. The isotope shift measured in our study can be compared with that using the mean square charge radii difference $\delta\langle r^2 \rangle$ data [13]. The difference $\delta\langle r^2 \rangle$ for ^{175}Lu and ^{177}Lu exceeds that for ^{175}Lu and ^{176}Lu by about three times. This means that the isotope shift of ^{177}Lu relative to ^{175}Lu should be three times greater than that between ^{176}Lu and ^{175}Lu [25]. Taking as a reference the isotope shift between ^{176}Lu and ^{175}Lu as −388.8 MHz [12], we obtain in this case an isotope shift between ^{177}Lu and ^{175}Lu of −1147 MHz. Analogous estimates of constants and isotope shifts can be made for the ^{177m}Lu isomer (Table 2).

The relative positions of the studied ^{177}Lu HFS components and those calculated for the natural isotopes are shown on the common frequency scale (Fig. 5). Calculations were made using the literature values for the constants [12, 13, 23, 26].

Figure 5 shows that transitions $2 \rightarrow 1$, $2 \rightarrow 3$, $3 \rightarrow 3$, $4 \rightarrow 3$, $4 \rightarrow 5$, and $5 \rightarrow 6$ are suitable for ^{177}Lu selective photoionization because these components are well separated from the components of the other isotopes.

The result of ^{177}Lu selective photoionization on the 5–6 first transition is shown in Fig. 6. The mass spectrum was recorded at the wavelength of the first transition tuned to resonance with the 5–6 component, while the second- and third-stage wavelengths were tuned to the maximum current of ^{177}Lu. After wavelength adjustment, the mass spectrometer (resolving power at 10 % of peak height was 200) was scanned over the mass range of 170–180 a.m.u and the spectra were recorded. The first-, second-, and third-step laser average power densities were 10, 10 mW/cm^2, and 3.1 W/cm^2, respectively.

The selectivity of photoionization depended strongly on the first- and second-step laser intensities, the ^{177}Lu concentration being reduced to ~6 % for the first and second
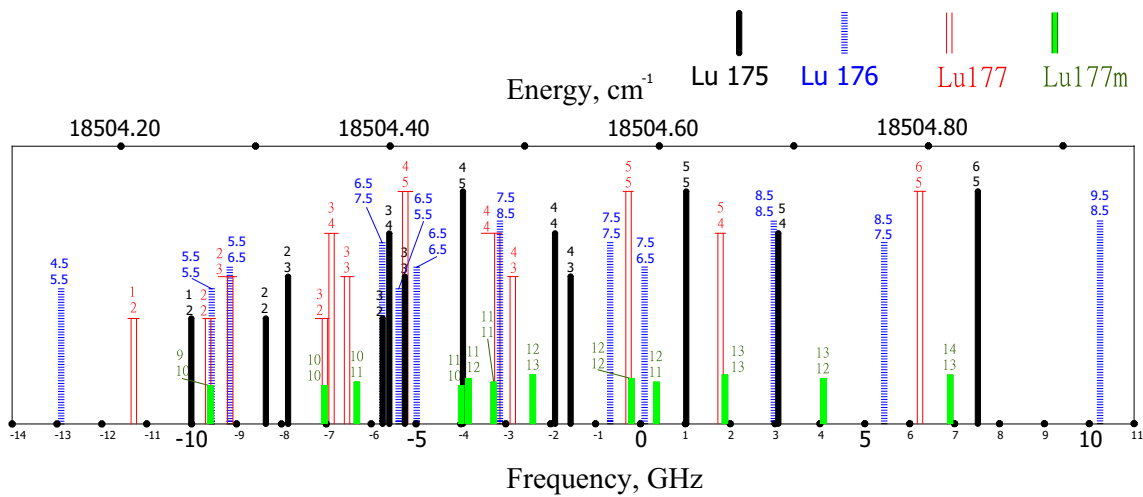
Fig. 5 Hyperfine spectral lines of lutetium isotopes. Frequency plotted on *horizontal axis* in GHz. Intensities are proportional to the population of the initial level regardless of isotope concentration. Zero on the scale is the position of the ^{175}Lu CG energy
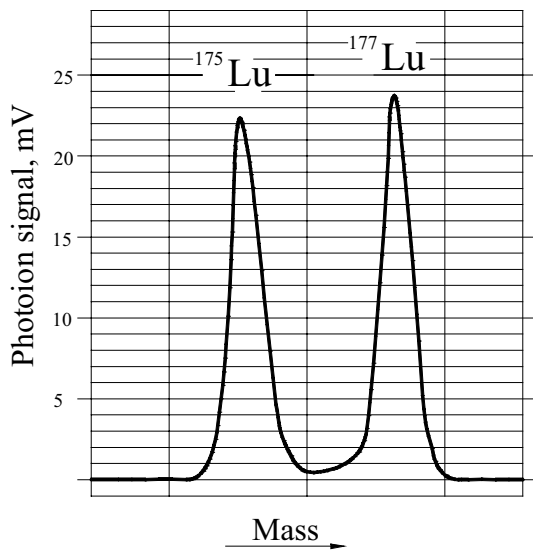

Fig. 6 Laser-induced photoion mass spectrum. *Vertical bar* is photoion signal, mV. Radiation at the first stage was tuned to resonance with component 5–6. The initial ^{177}Lu concentration was 10^{-5}. The first-, second-, and third-step laser average power densities were 10, 10 mW/cm^2, and 3.1 W/cm^2, respectively

laser average power densities of 20 and 300 mW/cm^2, respectively. The selectivity factor generally used in separation techniques can be represented as the ratio of the photoionization probability for the target isotope W_{177} and the non-target isotope W:

$$S = \frac{W_{177}}{W}. \qquad (2)$$

The number of target photoions is $W_{177} \cdot C_{F177}$, where C_{F177} is the initial concentration of the target isotope.

The number of non-target photoions is $W(1 - C_{F177})$. The photoion concentration of the target isotope measured by the mass spectrometer is therefore:

$$C_{P177} = \frac{W_{177} \cdot C_{F177}}{W_{177} \cdot C_{F177} + W(1 - C_{F177})}. \qquad (3)$$

Selectivity may be expressed in terms of concentrations by the formula:

$$S = \frac{W_{177}}{W} = \frac{C_{P177} \cdot (1 - C_{F177})}{(1 - C_{P177}) \cdot C_{F177}}. \qquad (4)$$

For a ^{177}Lu initial sample concentration $C_{F177} = 10^{-5}$ and a ^{177}Lu photoion concentration $C_{P177} = 0.5$, the selectivity (4) is 10^5. The selectivity measured exceeded significantly the ratio of the first-step laser intensities applied to the ^{177}Lu and ^{175}Lu isotopes. For the 5–6 transition (Fig. 5), the shift between the ^{177}Lu and ^{175}Lu components was 1300 MHz. The ratio of the Voigt intensity (with Lorentzian width 10 MHz and Gaussian width 125 MHz) at the center of the line to the intensity at a frequency of 1300 MHz from the center was 8×10^3. This excess selectivity may be explained by the additional selectivity at the second step. This finding is in good agreement with the experimental result that selectivity strongly depends on the second laser wavelength and intensity. The effect of improved selectivity by multistep ionization has been demonstrated by several groups [10, 27, 28].

The upper limit of photoionization efficiency may be determined by measuring the dependence of the photoion signal on laser intensity. A typical response curve showed a linear increase in photoion signal at low laser intensity, but with a further increase in intensity, the photoion signal became saturated. The reason for saturation is owing to a depletion of ground-state atoms. Figure 7 shows the
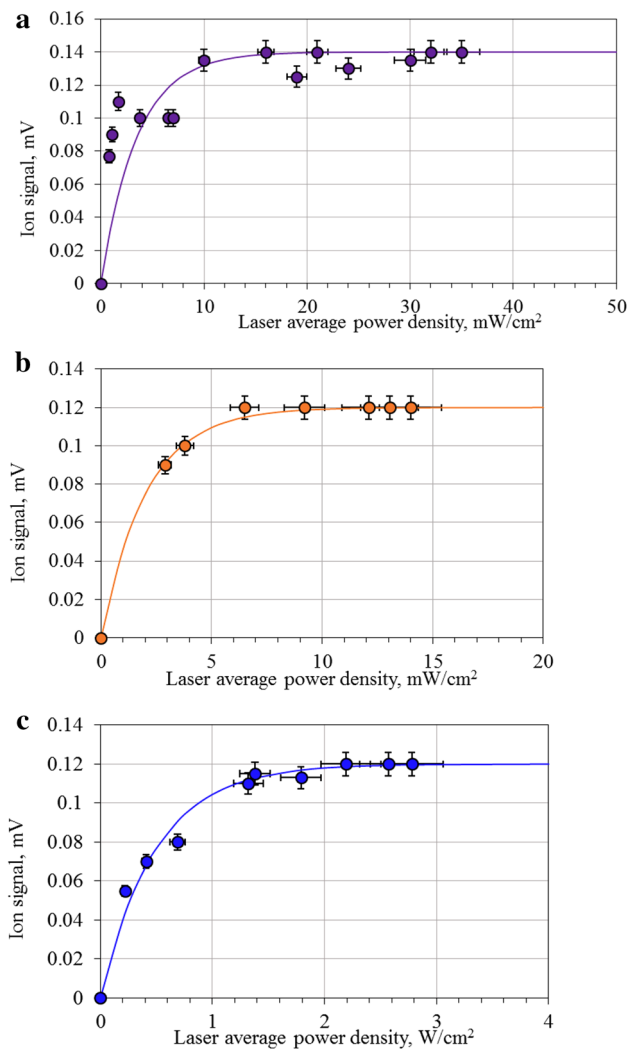
Fig. 7 **a** Dependence of ion signal on first-step laser intensity. The second- and third-step laser average power densities were 0.47 and 3.1 W/cm². **b** Dependence of ion signal on second-step laser intensity. The first- and third-step laser average power densities were 10 mW/cm² and 3.1 W/cm². **c** Dependence of ion signal on third-step laser intensity. The first- and second-step laser average power densities were 10 and 20 mW/cm²

Fig. 8 Concentration of ^{177}Lu in irradiated sample multiplied by 10^4 (*black line*). ^{177}Lu photoion concentration given by expression (4) with a selectivity of 10^5 (*red line*)

experimental dependence of photoion signal on the first (a)-, second (b)-, and third (c)-stage laser intensity. It can be seen that saturation was readily attained for 10 mW/cm² average power density at the first stage and 10 mW/cm² and 2 W/cm² at the second and third stages, respectively. In the case of saturation, the photoionization efficiency was proportional to the population of the start level. The ^{177}Lu ground-state population at the vaporization temperature of ~1700 K was 77 %. The ground state consists of four sublevels with F quantum numbers 2, 3, 4, and 5. The population of the sublevels is proportional to the statistical weight $2F + 1$ of the sublevel, i.e., 15.6, 21.9, 28.1, and 34.3 % for the sublevel with $F = 2, 3, 4$, and 5, respectively. For
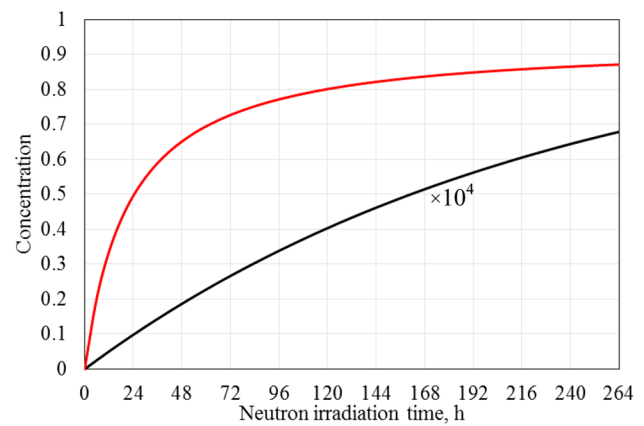
example, if the $F = 5$ sublevel is used as the initial level, the 34.3·0.77 ~26 % of ^{177}Lu atoms may be converted into photoions.

In the case of the second and third stages of photoionization where there is a 25-ns delay, a smaller portion of atoms may be ionized. This portion is equal to the amount of atoms that remained in the first excited state after the first-step pulse. This amount, in the case of saturation, is equal to the ratio of the statistical weight of the upper state to the statistical weight of the lower state. For the 5–6 transition, this ratio is 0.54 and the portion of ^{177}Lu atoms is reduced to ~14 %.

The remarkable feature of ^{177}Lu extraction technology is that it does not require significant mass productivity, in contrast to, for example, AVLIS for the production of 100 kg of ^{150}Nd [9]. The mass equivalent for a typical patient dose of 7 GBq is ~1.8×10^{-6} g of pure ^{177}Lu. This makes it possible to consider a production facility with the Doppler broadening of atom flow similar to that used in spectroscopic experiments to maintain the selectivity of photoionization. The many problems associated with ion extraction and ion sputtering disappears because of the low photoion current and extraction voltage. One source of loss, however, does remain, and this is connected with the probability of atom irradiation by the pulsed laser. This type of loss may be significantly reduced by stretching the laser irradiation volume along the atom flow. Therefore, it is reasonable to expect that the total extraction of ^{177}Lu in a production facility will be not less than 10 %.

Given that selectivity is invariant to variations in concentration, expression (4) may be used for the calculation of the ^{177}Lu photoion concentration, C_{P177}, at different initial concentrations C_{F177}. The result of the calculation is presented in Fig. 8 as a function of the sample neutron irradiation time.

The black line represents the dynamics of the production of ^{177}Lu concentration in an IR-8 reactor at a thermal neutron flux of 1.5×10^{13} 1/cm^{2}s. The red line is the calculation of the photoion ^{177}Lu concentration, C_{P177}, given by expression (4) with a selectivity of 10^5. The figure shows that even in the case of a relatively low neutron flux facility, it is possible to obtain a photoion ^{177}Lu concentration above 80 %. A selectivity of 10^5 is achieved at laser saturation intensities that permit significant photoionization efficiency, suitable for the technological applications.

An important advantage of the indirect route for ^{177}Lu production is the low content of ^{177m}Lu. The metastable isomer ^{177m}Lu with a decay half-life of 160 days complicates radioactive waste handling in medical practice. A typical value for the ^{177m}Lu/^{177}Lu ratio for the direct route varies between 0.01 and 0.02 % [6]. The AVLIS extraction of ^{177}Lu from a neutron-irradiated natural lutetium target has the potential for additional purification of ^{177m}Lu because the absorption lines of ^{177m}Lu (according to estimates in Table 2) are shifted from the ^{177}Lu lines by 670 MHz for the 5–6 transition and by 1700 MHz for the 2–1 transition.

4 Conclusions

The measurement of hyperfine structure and isotope shift for the $5d6s^2\ ^2D_{3/2} \to 5d6s6p\ ^4F_{5/2}$ transition revealed ^{177}Lu HFS components with a significant gap of ~1 GHz from the other isotopes. These spectral lines can be employed for the extraction of ^{177}Lu from an isotope mixture of irradiated natural lutetium by the AVLIS method. Experimentally, a selectivity of ^{177}Lu photoionization of 10^5 was achieved. The photoion concentration of ^{177}Lu of 50 % was obtained for irradiation of a natural lutetium sample for 1 day in a neutron flux of 1.5×10^{13} 1/cm^{2}s. The high ^{177}Lu photoion concentration occurred at laser intensities corresponding to the photoion current saturation range, and this is a good basis for further refinement and development of the separation technology.

References

1. NuPECC Report "Nuclear Physics for Medicine": 136 (2014)
2. D.J. Kwekkeboom, W.W. de Herder, B.L. Kam, C.H. van Eijck, M. van Essen, P.P. Kooij, R.A. Feelders, M.O. van Aken, E.P. Krenning, J. Clin. Oncol. **26**, 2124 (2008)
3. S. Khan, E.P. Krenning, M. van Essen, B.L. Kam, J.J. Teunissen, D.J. Kwekkeboom, J. Nucl. Med. **52**, 1361 (2011)
4. A. Dash, M.R.A. Pillai, F.F. Knapp Jr., Nucl. Med. Mol. Imaging **49**, 85 (2015). doi:10.1007/s13139-014-0315-z
5. W.A. Breeman, R.A. de Zanger, H.S. Chan, E. Blois, Curr. Radiopharm. **8**(2), 119–122 (2015)
6. R. Henkelmann, A. Hey, O. Buck, K. Zhernosekov, T. Nikula, Workshop "Physics for health in Europe", Contribution ID: 82 (2010)
7. J.A. Paisner, Appl. Phys. B **46**, 253 (1988)
8. P.T. Greenland, Contemp. Phys. **31**, 405 (1990)
9. A.P. Babichev, I.S. Grigoriev, A.I. Grigoriev, A.P. Dorovskii, A.B. D'yachkov, S.K. Kovalevich, V.A. Kochetov, V.A. Kuznetsov, V.P. Labozin, A.V. Matrakhov, S.M. Mironov, S.A. Nikulin, A.V. Pesnya, N.I. Timofeev, V.A. Firsov, G.O. Tsvetkov, G.G. Shatalova, Quantum Electron. **35**, 879 (2005). doi:10.1070/QE2005v035n10ABEH006601
10. H. Park, D.H. Kwon, Y.H. Cha, T.S. Kim, J. Han, K.H. Kon, D.Y. Jeong, C.J. Kim, J. Nucl. Sci. Techn. Supp. **6**, 111 (2008)
11. A. D'yachkov, S. Kovalevich, A. Labozin, S. Mironov, V. Panchenko, V. Firsov, G. Tsvetkov, G. Shatalova, Quantum Electron. **42**, 953 (2012). doi:10.1070/QE2012v042n10ABEH014929
12. W. Jin, M. Wakasugi, T. Inamura, T. Murayama, T. Wakui, H. Katsuragawa, T. Ariga, T. Ishizuka, M. Koizumi, I. Sugai, Phys. Rev. A **49**, 762 (1994). doi:10.1103/PhysRevA.49.762
13. U. Georg, W. Borchers, M. Keim, A. Klein, P. Lievens, R. Neugart, M. Neuroth, P.M. Rao, Ch. Schulz, the ISOLDE Collaboration, Eur. Phys. J. A **3**, 225 (1998)
14. F.R. Petersen, H.A. Shugart, Phys. Rev. **126**, 252 (1962)
15. R. Müller, E.W. Weber, Z. Physik A **275**, 305 (1975). doi:10.1007/BF01434016
16. S. Rothe, A.N. Andreyev, S. Antalic, A. Borschevsky, L. Capponi, T.E. Cocolios, H. De Witte, E. Eliav, D.V. Fedorov, V.N. Fedosseev, D.A. Fink, S. Fritzsche, L. Ghys, M. Huyse, N. Imai, U. Kaldor, Y. Kudryavtsev, U. Köster, J.F.W. Lane, J. Lassen, V. Liberati, K.M. Lynch, B.A. Marsh, K. Nishio, D. Pauwels, V. Pershina, L. Popescu, T.J. Procter, D. Radulov, E. Rapisarda, R.E. Rossel, K. Sandhu, M.D. Seliverstov, A.M. Sjödin, P. Van den Bergh, P. Van Duppen, M. Venhart, Y. Wakabayashi, K.D.A. Wendt, Nat. Commun. **4**, 1835 (2013). doi:10.1038/ncomms2819
17. B.L. Feary, D.C. Parent, R.A. Keller, C.M. Miller, J. Opt. Soc. Am. B **7**, 3 (1990)
18. I. Grigoriev, A. Diachkov, V. Kuznetsov, V. Labosin, V. Firsov, in *Proceedings of SPIE 5121 Laser Processing of Advanced Materials and Laser Microtechnologies* 411 (2003)
19. I. Grigoriev, A. D'yachkov, V. Labozin, S. Mironov, S. Nikulin, V. Firsov, Quantum Electron. **34**, 447 (2004)
20. J.A. Fedchak, E.A. Den Hartog, J.E. Lawler, P. Palmeri, P. Quinet, E. Biemont, Astrophys. J. **542**, 1109 (2000)
21. http://cernlibweb.cern.ch/cernlib
22. I. Sobelman, *Introduction to theory of atomic spectra (in Russian)* (Nauka, Moscow, 1977)
23. A. Kuhnert, A. Nunnemann, D. Zimmermann, J. Phys. B **16**, 4299 (1983). doi:10.1088/0022-3700/16/23/013
24. S. Witte, E. van Duijn, R. Zinkstok, W. Hogervorst, Eur. Phys. J. D **20**, 159 (2002)
25. L. Landau, E. Lifshitz, *Quantum Mechanics*, vol. 3 (Pergamon Press, New York, 1965)
26. J. Verges, J.F. Wyart, Phys. Scripta **17**, 495 (1978)
27. B.A. Bushaw, W. Nörtenhäuser, K. Wendt, Spectrochim. Acta B **54**, 321 (1999)
28. P. Müller, B.A. Bushaw, K. Blaum, S. Diel, Ch. Geppert, A. Nähler, N. Trautmann, W. Nörtenhäuser, K. Wendt, Fresenius J. Anal. Chem. **370**, 508 (2001)